Histone Demethylase Inhibition

DOI: 10.1002/ange.201107833

Linking of 2-Oxoglutarate and Substrate Binding Sites Enables Potent and Highly Selective Inhibition of JmjC Histone Demethylases**

*Esther C. Y. Woon, Anthony Tumber, Akane Kawamura, Lars Hillringhaus, Wei Ge, Nathan R. Rose, Jerome H. Y. Ma, Mun Chiang Chan, Louise J. Walport, Ka Hing Che, Stanley S. Ng, Brian D. Marsden, Udo Oppermann, Michael A. McDonough, and Christopher J. Schofield**

N^{ε}-Methylation of histone lysine residues is an "epigenetic modification" that can be either transcriptionally activating or deactivating, depending on the position of the lysine, its methylation state and the presence of other modifications.[1] The largest family of demethylases, the JmjC enzymes, employ 2-oxoglutarate (2OG) as a cosubstrate (Figure 1 a).[2,3] Some JmjC demethylases are targeted for cancer treatment[4–6] and inflammatory diseases.[7] There are 5 JmjC demethylase subfamilies, targeting histone lysines (H3K = histone 3 lysine-residue) including at H3K4, H3K9, H3K27, and H3K36 (Figure 1 b). The factors determining JmjC selectivities are emerging, and involve both catalytic[8–10] and non-catalytic domains.[11–13] Although there are reports of JmjC inhibitors,[14–19] to date there are no reported compounds that are selective for subfamilies/isoforms. Here we report that a strategy involving binding to both the 2OG and substrate binding sites leads to selective and potent inhibitors of the JMJD2 subfamily.

There are predicted to be four human JMJD2 enzymes (A to D) and a "pseudogene" product JMJD2E. JMJD2A–C accept both H3K9me3/me2 and H3K36me3/me2, whereas JMJD2D–E only accept H3K9me3/me2.[20] Most, if not all, reported JmjC inhibitors are 2OG analogues with limited or undetermined selectivity, and with the exception of some peptide-based inhibitors,[14] have not, at least rationally, exploited the histone binding pocket.[14,21] We reasoned that "two-component inhibitors" that bind to 2OG and histone

a)

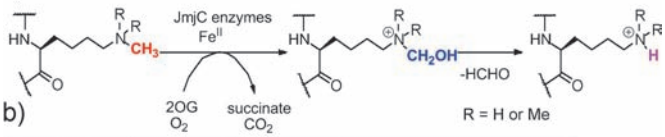

b)

JmjC Subfamilies	Members	Synonyms	Substrate Specificity
KDM2/7	KDM2A	FBXL11	H3K36me2/1
	KDM2A	FBXL10	
	KDM7A	KIAA1718	H3K27me2/1
		PHF8	H3K9me2/1, K36me2, H3K27me2/1, H4K20me1
KDM3	KDM3A	JMJD1A	H3K9me2/1
	KDM3B	JMJD1B	
	KDM3C	JMJD1C	
KDM4	KDM4A	JMJD2A	H3K9me3/2 H3K36me3/2
	KDM4B	JMJD2B	
	KDM4C	JMJD2C	
	KDM4D	JMJD2D	H3K9me3/2
	KDM4E	JMJD2E	
KDM5	KDM5A	JARID1A	H3K4me3/2/1
	KDM5B	JARID1B	
	KDM5C	JARID1C	
KDM6	KDM6A	UTX	H3K27me3/2/1
	KDM6B	JMJD3	

c)

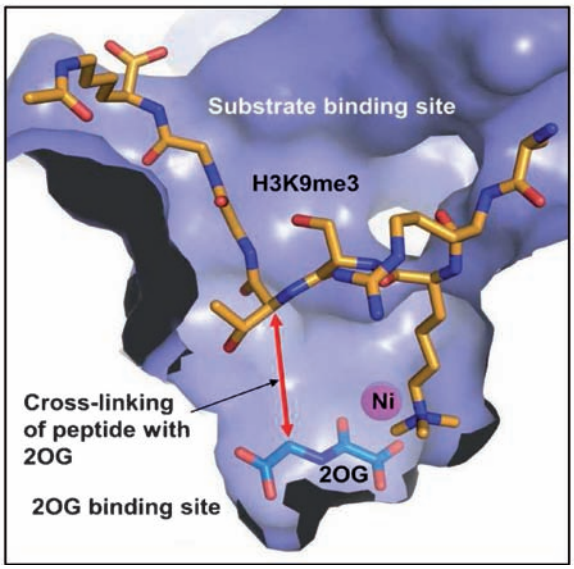

Figure 1. The JmjC histone demethylases. a) Reactions catalyzed by JmjC enzymes. b) Members of the five assigned subfamilies of human JmjC enzymes. Substrate assignments are in progress for some members. c) Active-site view from a crystal structure of JMJD2A bound to a H3K9me3 fragment (orange) and 2OG (blue) (PDB ID 2Q8C).[9] The cross-linking point identified by mass spectrometric studies (Figure 2) is shown by the red arrow.

[*] Dr. E. C. Y. Woon,[+] Dr. A. Kawamura, Dr. L. Hillringhaus, Dr. W. Ge, Dr. N. R. Rose, J. H. Y. Ma, M. C. Chan, L. J. Walport, Dr. M. A. McDonough, Prof. C. J. Schofield
Chemistry Research Laboratory, University of Oxford
12 Mansfield Road, Oxford, OX1 3TA (UK)
E-mail: christopher.schofield@chem.ox.ac.uk

Dr. A. Tumber, K. H. Che, Dr. S. S. Ng, Dr. B. D. Marsden, Prof. U. Oppermann
Structural Genomics Consortium, University of Oxford
Old Road Campus Research Building, Oxford, OX3 7DQ (UK)

[+] Current address: Department of Pharmacy, National University of Singapore, 18 Science Drive 4, Singapore 117543 (Singapore)

[**] This work was supported by the Biotechnology and Biological Sciences Research Council, the Wellcome Trust, the European Research Council, the German Academic Exchange Service (DAAD) (L.H.), the European Union, and the Structural Genomics Consortium (registered charity no. 1097737).

Supporting information for this article is available on the WWW under http://dx.doi.org/10.1002/anie.201107833.

binding sites may enable selectivity (Figure 1c). In the design of JMJD2 selective inhibitors, we used DNOC **1** (*N*-oxalyl-D-cysteine), which chelates to the iron as the 2OG-binding component and substrate fragment H3K9me3 (7–14) as the substrate-binding component (Figure 2a). To identify a suitable cross-linking point, we employed the technique of dynamic chemistry linked to MS analysis using the reversible thiol–disulfide reaction (with multiple thiols, this is termed dynamic combinatorial mass spectrometry, DCMS). Non-denaturing electrospray ionization mass spectrometry (ESI-MS) is used to identify members of equilibrating disulfides that bind to the target protein.[17,22,23]

Analysis of JMJD2 structures[10] reveals a large pocket in which the 2OG and H3K binding sites are contiguous. Our approach to identifying a site for cross-linking involved substituting each of the residues proceeding the trimethylated lysine of a H3K9me3 fragment sequence (residues 7–14) with a Cys residue 10–13, Figure 2a, then using MS to analyze for cross-linking to DNOC **1** or LNOC **2** concomitant with binding to JMJD2E (which is amenable to non-denaturing MS analysis). The results reveal that only the combination of peptide T11C (i.e. Thr11 replaced with Cys) and DNOC **1** form an apparent disulfide **4**, capable of substantially binding to JMJD2E.Fe^{II} (hereafter JMJD2E, Figure 2b). No binding was observed for the other H3K9me3 cysteinyl variants: DNOC **1**/LNOC **2** combinations, implying a selection of **4** by JMJD2E.

Differential scanning fluorimetry ("thermal shift" T_m) assays[24] support the MS analyses, with large T_m shifts being observed for the T11C:**1** combination for JMJD2A (T_m shift = 9.5 °C) and JMJD2E (T_m shift = 13.2 °C); T11C or **1** alone gave insignificant T_m shifts (Figure 2c). No T_m shifts were observed for other combinations of cysteinyl peptides: DNOC **1**, LNOC **2**, or NOG **3** (*N*-oxalylglycine). No T_m shift was observed for the K9me2/me1/me0 T11C variants, including those with a longer H3K9me3(1–15) sequence (Figure 3a), implying binding of the trimethylated form is preferred for binding of the cross-linked molecules. In contrast, varying the methylation state at K4 of H3K9me3-(1–15) did not affect the T_m shift (Figure 3a). To study the effects of substrate length, residues surrounding the "Kme3SC motif" of the T11C peptides were systematically removed (Supporting Information, Figure S1). Tm shift analyses of these peptides with **1** in JMJD2A and JMJD2E imply both Ala7 and Arg8 of T11C/**4** are important for binding (Figure S1).

A structure for JMJD2A in complex with disulfide **4** (from DNOC **1** and T11C) (PDB ID 3U4S, Figure 3c, S2 and S3) reveals how 2OG and histone binding sites can be occupied simultaneously. When complexed with **1**, the active site metal (Ni^{II} for Fe^{II}) is coordinated by His188, Glu190 and His276 side chains. The *N*-oxalyl amide carbonyl oxygen and one of the carboxylate oxygens of **1** coordinate the metal bidentately, as does 2OG. The other carboxylate of **1** forms a salt bridge with Lys206 side-chain amine (2.8 Å) and hydrogen-bond with Tyr132 side-chain hydroxy (2.5 Å). Consistent with the binding studies (Figure S1), both Ala7 and Arg8 of T11C form apparently important interactions (Figure S2).

The T11C component of **4** adopts a "bent conformation" as observed for an H3K9me3 peptide fragment in complex with JMJD2A, which directs the *N*-trimethyl group. There is no significant difference in the conformations of the T11C (**4**) and H3K9me3 backbones (rmsd 0.3 Å), except for the side-chain position of Cys11 in T11C, which rotates by ca. 70° with respect to that of H3K9me3 Thr11 to enable disulfide formation with the thiol of **1**. Modeling suggests that only

a)

H3K9me3	ARK(me3)STGGK-NH_2
S10C	ARK(me3)C_{10}TGGK-NH_2
T11C	ARK(me3)SC_{11}GGK-NH_2
G12C	ARK(me3)STC_{12}GK-NH_2
G13C	ARK(me3)STGC_{13}K-NH_2

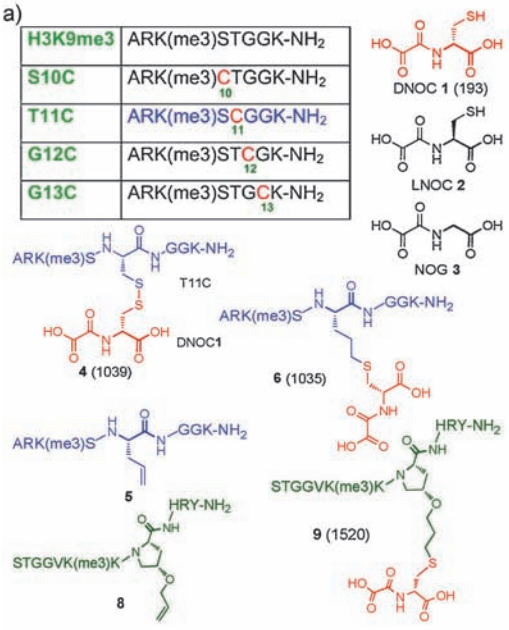

b)

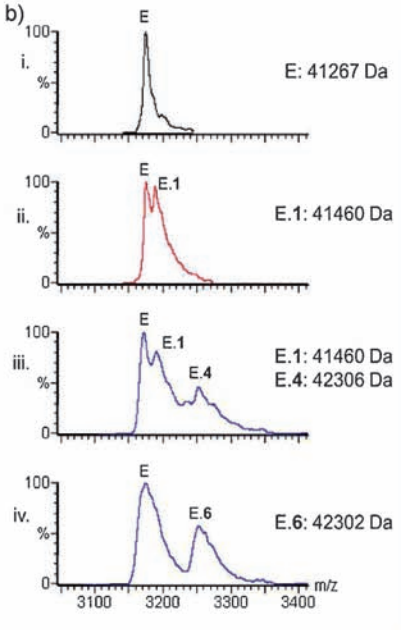

c)

		T_m shift/°C (JMJD2A)	T_m shift/°C (JMJD2E)
K9me3	1	1.0	-1.1
	2	0.6	-1.0
	3	1.0	-0.3
	-	-0.1	-0.2
S10C	1	2.0	-0.4
	2	0.8	-0.7
	3	2.2	0.2
	-	-0.1	-0.2
T11C	1	9.5	13.2
	2	0.8	0.3
	3	2.3	0.7
	-	0.1	-0.3
G12C	1	1.5	-0.4
	2	0.9	-0.8
	3	2.1	0.7
	-	0.1	0.3
G13C	1	1.1	-1.2
	2	0.3	-0.5
	3	2.2	0.9
	-	-0.2	-0.3
-	1	0.7	0.5
	2	0.3	0.3
	3	1.2	1.5

Figure 2. Mass spectrometric approach to identifying points for inhibitor–substrate cross-linking a) Sequences and structures of inhibitors. b) MS analyses on JMJD2E.Fe^{II} (labeled E, $z = 13$) in the presence of i) no compound, and compounds ii) *N*-oxalyl-D-cysteine **1**, iii) disulfides **4**, iv) cross-linked compound **6**. Masses (Da) in parentheses. c) Thermal shift with **1**–**3**.

a)

	T_m shift/ °C (JMJD2A)	T_m shift/ °C (JMJD2E)
ARK(me3)SCGGK (T11C)	9.5	13.2
ARK(me2)SCGGK	1.8	-0.4
ARK(me1)SCGGK	0.8	1.1
ARKSCGGK	0.1	0.2
ARTKQTARK(me3)SCGGKA	9.1	10.6
ARTKQTARK(me2)SCGGKA	0.1	-1.3
ARTKQTARK(me1)SCGGKA	0.3	0.2
ARTKQTARKSCGGKA	0.5	0.3
ARTK(me3)QTARK(me3)SCGGKA	8.5	9.5
ARTK(me2)QTARK(me3)SCGGKA	8.8	9.6
ARTK(me1)QTARK(me3)SCGGKA	8.7	9.5

b)

	6		9	
	IC_{50}/ µM	T_m shift/ °C	IC_{50}/ µM	T_m shift/ °C
JMJD1A	>100	-0.3	60	-0.1
JMJD2A	0.27	7.1	1.5	5.8
JMJD2E	0.09	12.1	91	0.5
JMJD3	>100	0.1	NI_{100}	0.2
FBXL11	NI_{100}	0.2	55	0.9
PHF8	1000	-0.3	>1000	-0.3
PHD2	>500	0.2	>200	0.2
FIH	>1000	0.2	>1000	-0.5

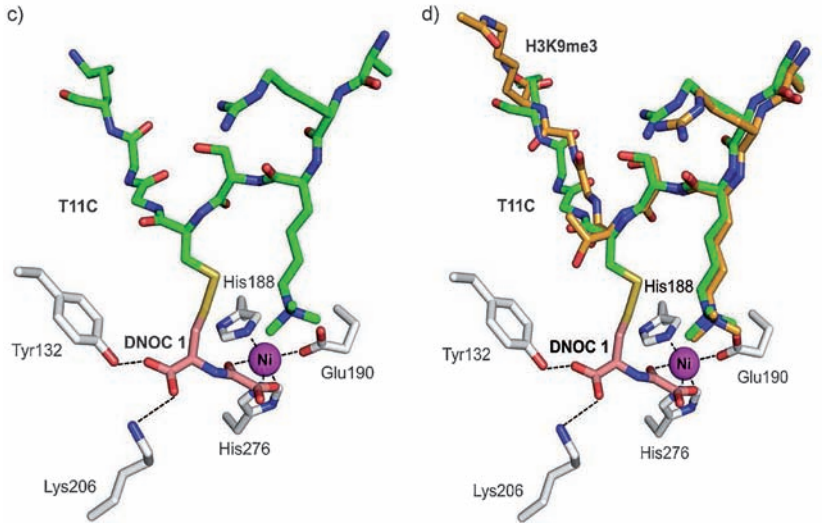

Figure 3. Selective inhibition of JMJD2A and JMJD2E. a) T_m shift studies of disulfide cross-linking of DNOC **1** to T11C variants. b) Selectivity studies of **6** and **9** against representatives of JmjC demethylases, PHD2 and FIH; NI_{100} = no inhibition at 100 µM. c) View from a JMJD2A structure (white) bound to T11C (green) and DNOC **1** (salmon) (PDB ID 3U4S). d) Superimposition of a view from a JMJD2A:T11C:**1** structure with that of a structure of JMJD2A complexed with H3K9me3 (orange) (PDB ID 2OQ6, Ni^{II} substituting for Fe^{II}).[10]

Thr11 in H3K9me3 is correctly positioned for reaction with DNOC **1**; cross-linking is not possible with cysteine replacement at H3K9me3 Ser10, Gly12 or Gly13 (Figure 2). Notably, the Lys14 side-chain position of T11C (**4**) is rotated by ca. 95° with respect to its position in H3K9me3; this directs the amide of Gly13 in T11C (**4**) away from the backbone oxygen of $His240_{JMJD2A}$, weakening the hydrogen bond between them compared to that with Gly13 of H3K9me3 (Figure S4). $His240_{JMJD2A}$ coordinates an ion zinc, the binding of which is proposed as important for substrate recognition by the JMJD2 subfamily.[10,21]

We synthesized a stable analogue of the T11C:**1** disulfide **4**, wherein the disulfide is replaced with a CH_2–S bond, using a thiol–ene coupling as a key step,[25] i.e. addition of a thinyl radical to an allylglycine-containing peptide **5** (Scheme 1a; Supporting Information). The analogue **6** binds strongly to JMJD2E by ESI-MS (Figure 2b); Kinetic analyses[18] reveal a mixed mode of inhibition of JMJD2E by **6** with respect to 2OG ($K_i^{app} = 114 \pm 46$ nM, $\alpha = 2.3 \pm 1.4$), suggesting it binds both JMJD2E and JMJD2E.2OG (Figure S5a). No demethylation of **6** by JMJD2E was observed by MALDI-MS[10] in the presence of 2OG; T11C alone showed < 5% demethylation by JMJD2E under these conditions (Figure S5b).

Profiling studies using luminescence assays[26] and T_m analyses revealed selectivity of **6** for the JMJD2 subfamily; **6** potently inhibits both JMJD2A ($IC_{50} = 0.27$ µM, $T_m = +7.1$ °C) and JMJD2E ($IC_{50} = 0.09$ µM, $T_m = +12.1$ °C), with little or no inhibition or T_m shift against other JmjC subfamilies (Figure 3b and S6a). The JMJD1A results are notable because it also acts on H3K9. T_m assays were carried out for the K9me3/me2/me1/me0 Cys variants of H3K9 (1–15) in the presence of **1** for JMJD1A; in all cases, no T_m shifts were observed for the cross-linked compounds (Figure S7a). Similarly, no shifts were observed for the disulfides formed between **1** and K9me3/me2/me1/me0 cysteine variants of K4me3K9 (1–15) for PHF8, which acts on H3K9 (Figure S7b). **6** was also tested against PHD2 (hypoxia-inducible factor prolylhydroxylase 2, which is central to the hypoxic response)[3] and FIH (factor inhibiting hypoxia inducible factor)[3] with IC_{50} values > 500 µM and > 1 mM, respectively (Figure 3a). **6** is thus, in our assays, > 300-fold selective for JMJD2A over the other 2OG oxygenases tested (Figure 1b).

The T_m results revealed that the K9me3 form of the cross-linked inhibitor (as in **6**) is the preferred methylation state form for inhibition (Figure 3a). This may reflect the proximity of the cross-linking and the methylated lysine arm as revealed in the structure (Figure 3c). In the selectivity studies, JmjC demethylases with varying methylation state and sequence selectivities (H3K9, H3K27, H3K36) were tested. Note that no inhibition of JMJD1A and PHF8 were observed; both these enzymes, like the JMJD2 subfamily, act on H3K9, but prefer Kme2 (Figure 1b). The results thus demonstrate that the selectivities of **4** and **6**

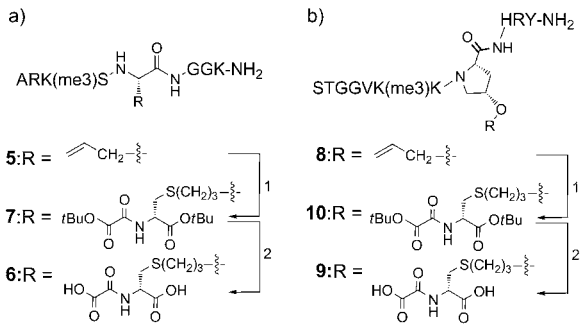

Scheme 1. Synthesis of stable carbon analogue a) **6** and b) **9** by utilizing a thiol–ene coupling reaction. Reagents and conditions: 1) Dimethoxyphenyl acetophenone, anhydrous MeOH, *hν* (365 nm, 2 h); 2) 30% (v/v) CF_3CO_2H/CH_2Cl_2, RT (3 h).

arise from active-site structure coupled to sequence and methylation state selectivity.

We investigated whether we could design JMJD2 isoform-group selective inhibitors, using JMJD2A and JMJD2E as representatives. JMJD2A–C accept both H3K9me3/me2 and H3K36me3/me2 whereas JMJD2D–E only accept H3K9me3/me2. We proposed that a H3K36-based inhibitor might select for JMJD2A over JMJD2E. Modeling of a JMJD2A:H3K36me3 structure suggests cross-linking of **1** with Pro38 of H3K36me3 (31–41) could be achieved (Figure S7). Synthesis of crossed-linked compound **9** was carried out by thiol–ene coupling of an *O*-allylhydroxyproline-containing peptide **8** with **1** (Scheme 1b). **9** demonstrated 60-fold selectivity for JMJD2A ($IC_{50} = 1.5$ μM, T_m shift = 5.8 °C) over JMJD2E ($IC_{50} = 91$ μM, T_m shift < 1 °C) and **9** did not bind to JMJD2E by non-denaturing ESI-MS. There is little or no inhibitory activity or T_m shift of **9** against the other tested JmjC subfamilies (Figure 3b and S6b). Notably, **9** showed >35-fold selectivity against FBXL11 ($IC_{50} = 55$ μM, T_m shift = 0.9 °C) and >650-fold selectivity against PHF8 ($IC_{50} > 1$ mM, T_m shift = −0.3 °C).

Overall the results provide proof of principle that selective inhibition of not only JmjC subfamilies, but also isoform subgroups, is achievable by utilizing both 2OG and substrate binding sites. With use of an appropriately functional inhibitor, the cross-linking approach should be applicable to other 2OG oxygenase subfamilies. By exploiting the inherent substrate selectivity of the JmjC enzymes, compound **6**, which is based on H3K9me3, exhibits a high degree of selectivity and potency for the JMJD2 over other JmjC subfamilies. Discrimination against human 2OG oxygenases should be possible as shown by a lack of inhibition against PHD2 and FIH. Importantly, isoform-subgroup selectivity could also be achieved using this strategy, as demonstrated by **9** which is selective for JMJD2A over JMJD2E. It is likely that the approach outlined here will be applicable to related histone demethylases, and, more widely, other 2OG oxygenases. The combined results, including crystallographic analyses, should provide a basis for the development of potent and selective JmjC inhibitors, suitable for use as functional probes in cells and, possibly, for clinical use.

Experimental Section

Experimental details, including syntheses and characterizations, ESI-MS methods, thermal shift and inhibition assays, protein purifications, crystallization and structure solutions, are given in the Supporting Information. The coordinates for JMJD2A in complex with T11C and DNOC **1** is deposited as PDB ID 3U4S.

Received: November 7, 2011
Published online: January 12, 2012

Keywords: 2-oxoglutarate · epigenetics · histone lysine demethylases · oxygenases · thiol–ene reaction

[1] R. J. Klose, E. M. Kallin, Y. Zhang, *Nat. Rev. Genet.* **2006**, *7*, 715–727.
[2] C. Martin, Y. Zhang, *Nat. Rev. Mol. Cell Biol.* **2005**, *6*, 838–849.
[3] N. R. Rose, M. A. McDonough, O. N. King, A. Kawamura, C. J. Schofield, *Chem. Soc. Rev.* **2011**, *40*, 4364–4397.
[4] J. He, A. T. Nguyen, Y. Zhang, *Blood* **2011**, *117*, 3869–3880.
[5] J. Yang, A. M. Jubb, L. Pike, F. M. Buffa, H. Turley, D. Baban, R. Leek, K. C. Gatter, J. Ragoussis, A. L. Harris, *Cancer Res.* **2010**, *70*, 6456–6466.
[6] P. A. Cloos, J. Christensen, K. Agger, A. Maiolica, J. Rappsilber, T. Antal, K. H. Hansen, K. Helin, *Nature* **2006**, *442*, 307–311.
[7] F. De Santa, M. G. Totaro, E. Prosperini, S. Notarbartolo, G. Testa, G. Natoli, *Cell* **2007**, *130*, 1083–1094.
[8] J. F. Couture, E. Collazo, P. A. Ortiz-Tello, J. S. Brunzelle, R. C. Trievel, *Nat. Struct. Mol. Biol.* **2007**, *14*, 689–695.
[9] Z. Chen, J. Zang, J. Kappler, X. Hong, F. Crawford, Q. Wang, F. Lan, C. Jiang, J. Whetstine, S. Dai, K. Hansen, Y. Shi, G. Zhang, *Proc. Natl. Acad. Sci. USA* **2007**, *104*, 10818–10823.
[10] S. S. Ng, K. L. Kavanagh, M. A. McDonough, D. Butler, E. S. Pilka, B. M. Lienard, J. E. Bray, P. Savitsky, O. Gileadi, F. von Delft, N. R. Rose, J. Offer, J. C. Scheinost, T. Borowski, M. Sundstrom, C. J. Schofield, U. Oppermann, *Nature* **2007**, *448*, 87–91.
[11] J. R. Horton, A. K. Upadhyay, H. H. Qi, X. Zhang, Y. Shi, X. Cheng, *Nat. Struct. Mol. Biol.* **2010**, *17*, 38–43.
[12] C. Loenarz, W. Ge, M. L. Coleman, N. R. Rose, C. D. O. Cooper, R. J. Klose, P. J. Ratcliffe, C. J. Schofield, *Hum. Mol. Genet.* **2010**, *19*, 217–222.
[13] L. Hillringhaus, W. W. Yue, N. R. Rose, S. S. Ng, C. Gileadi, C. Loenarz, S. H. Bello, J. E. Bray, C. J. Schofield, U. Oppermann, *J. Biol. Chem.* **2011**, DOI: 10.1074/jbc.M11.283689.
[14] B. Lohse, A. L. Nielsen, J. B. L. Kristensen, C. Helgstrand, P. A. C. Cloos, L. Olsen, M. Gajhede, R. P. Clausen, J. L. Kristensen, *Angew. Chem.* **2011**, *123*, 9266–9269; *Angew. Chem. Int. Ed.* **2011**, *50*, 9100–9103.
[15] X. Luo, Y. Liu, S. Kubicek, J. Myllyharju, A. Tumber, S. Ng, K. H. Che, J. Podoll, T. D. Heightman, U. Oppermann, S. L. Schreiber, X. Wang, *J. Am. Chem. Soc.* **2011**, *133*, 9451–9456.
[16] K. H. Chang, O. N. King, A. Tumber, E. C. Y. Woon, T. D. Heightman, M. A. McDonough, C. J. Schofield, N. R. Rose, *ChemMedChem* **2011**, *6*, 759–764.
[17] N. R. Rose, E. C. Y. Woon, G. L. Kingham, O. N. F. King, J. Mecinović, I. J. Clifton, S. S. Ng, J. Talib-Hardy, U. Oppermann, M. A. McDonough, C. J. Schofield, *J. Med. Chem.* **2010**, *53*, 1810–1818.
[18] N. R. Rose, S. S. Ng, J. Mecinović, B. M. Liénard, S. H. Bello, Z. Sun, M. A. McDonough, U. Oppermann, C. J. Schofield, *J. Med. Chem.* **2008**, *51*, 7053–7056.
[19] S. Hamada, T. Suzuki, K. Mino, K. Koseki, F. Oehme, I. Flamme, H. Ozasa, Y. Itoh, D. Ogasawara, H. Komaarashi, A. Kato, H. Tsumoto, H. Nakagawa, M. Hasegawa, R. Sasaki, T. Mizukami, N. Miyata, *J. Med. Chem.* **2010**, *53*, 5629–5638.
[20] J. R. Whetstine, A. Nottke, F. Lan, M. Huarte, S. Smolikov, Z. Chen, E. Spooner, E. Li, G. Zhang, M. Colaiacovo, Y. Shi, *Cell* **2006**, *125*, 467–481.
[21] R. Sekirnik, N. R. Rose, A. Thalhammer, P. T. Seden, J. Mecinović, C. J. Schofield, *Chem. Commun.* **2009**, 6376–6378.
[22] B. M. R. Liénard, R. Hüting, P. Lassaux, M. Galleni, J.-M. Frère, C. J. Schofield, *J. Med. Chem.* **2008**, *51*, 684–688.
[23] S.-A. Poulsen, *J. Am. Soc. Mass Spectrom.* **2006**, *17*, 1074–1080.
[24] F. H. Niesen, H. Berglund, M. Vedadi, *Nat. Protoc.* **2007**, *2*, 2212–2221.
[25] A. Dondoni, A. Massi, P. Nanni, A. Roda, *Chem. Eur. J.* **2009**, *15*, 11444–11449.
[26] A. Kawamura, A. Tumber, N. R. Rose, O. N. King, M. Daniel, U. Oppermann, T. D. Heightman, C. Schofield, *Anal. Biochem.* **2010**, *404*, 86–93.

